

Laboratori Nazionali di Frascati

LNF-68/68

F. Bordoni, T. Letardi and M. Placidi : BEAM EMITTANCE  
MEASUREMENTS ON THE FRASCATI 10 MeV MICROTRON.

Nuclear Instr. and Meth. 65, 72 (1968)

**BEAM EMITTANCE MEASUREMENTS ON THE FRASCATI 10 MeV MICROTRON**

F. BORDONI

*Università di Catania*

T. LETARDI and M. PLACIDI

*Laboratori Nazionali di Frascati del CNEN, Frascati, Rome, Italy*

Received 13 May 1968

In this note we describe a method used to measure the emittance of the beam from a 10 MeV microtron in operation at Laboratori Nazionali di Frascati.

A preliminary set of results, for the actual operating point of

the machine, is reported here. A systematic investigation will be carried out in the near future taking into account the features of the machine.

**1. Description of the method**

The method we adopted is the two-slit method<sup>1</sup>). It can be seen easily that with two parallel slits, separated by a zero-field drift space, it is possible to sample the area representing the beam in the phase plane (defined by the slits). To each position of the first slit corresponds an  $x$  limited portion of the area in the  $x-x'$  distribution of the beam emerging from the slit.

with respect to the slit (3) by means of the double steering coil system (2); the steering coils (4) can sweep the beam selected by (3) through the slit (3') followed by the beam detector.

A systematic error is introduced with this apparatus but it can be easily evaluated and corrected. Following the sketch of fig. 2, the ray  $R_0$  having an angle  $\alpha_0$  with respect to the system axis must be deflected by an angle

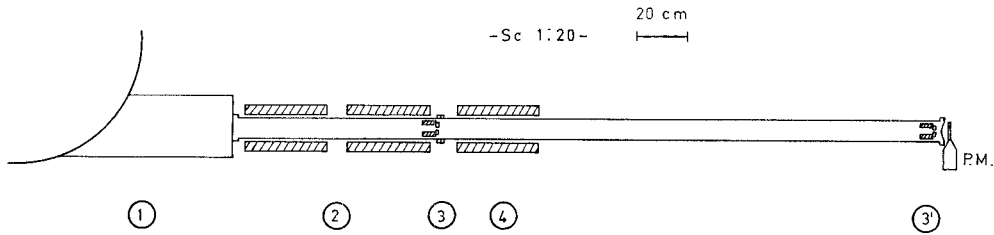


Fig. 1. Experimental apparatus.

In this method movable slits are needed. We modified the apparatus by using fixed slits and instead displacing the beam with steering coils, this yields both a simplification of the mechanics and a faster automatic scanning.

The experimental apparatus is shown in fig. 1. The 10 MeV beam from the microtron (1) can be displaced

$\alpha_t > \alpha_0$  to enter the slit (3'). It can be easily shown that  $\alpha_t$  is related to  $\alpha_0$  by the relation:

$$\alpha_0 = \alpha_t / \{1 + (L_1/L_2)\},$$

where  $\{1 + (L_1/L_2)\}$  is about 1.1.

In our case the beam detector is a small perspex slide (1 mm thick and 10 mm wide) viewed by an RCA type

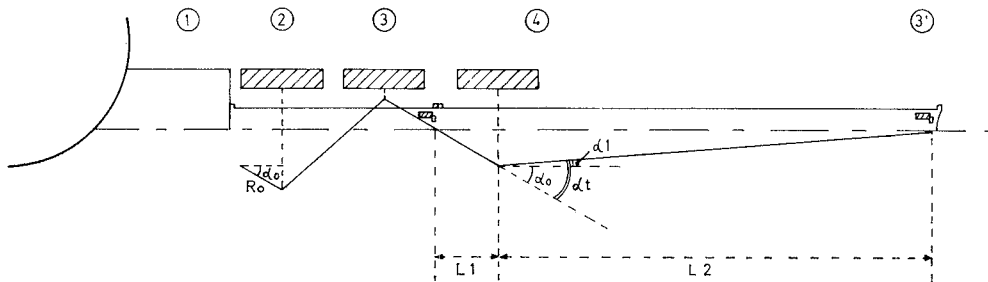


Fig. 2. Explaining the systematic error in the angular distribution.

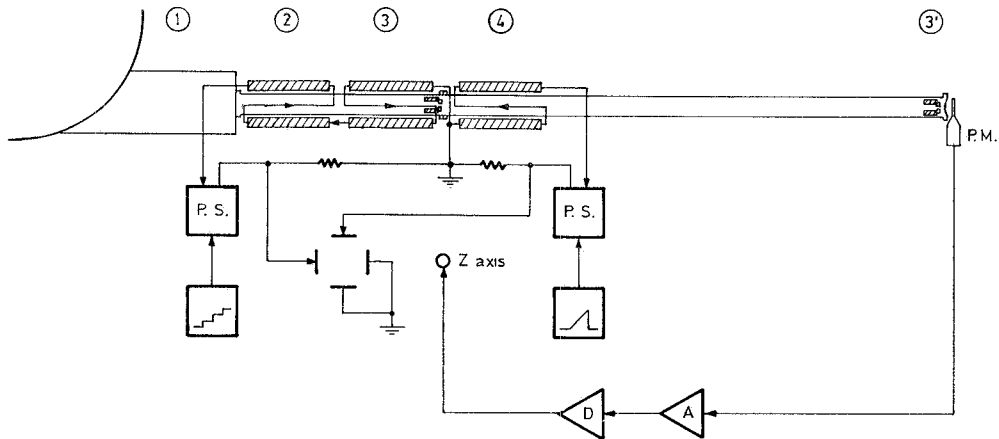


Fig. 3. Block diagram of the electronics.

931 photomultiplier operating in the linear region. To avoid saturation effects the last three dynodes have been short circuited.

The slits consisted of tungsten blocks supported by a lead frame and the aperture could be fixed at will. The tungsten thickness was 10 mm corresponding to 2.8 r.l.

The block diagram of associated electronics is shown in detail in fig. 3. Remotely programmable current power supplies were used for the steering coils. A voltage, proportional to the steering current, is applied to the  $x$  and  $y$  plates of the CRT, for the coils (2) and (4) respectively, while the  $z$ -axis is enhanced by the photomultiplier output; several levels of beam density are selected by means of the discriminator D. The current in the steering coils (2) is programmed with a

staircase function; at each step a sawtooth generator drives the supply for steering (4).

To obtain continuous scanning, the field strength in the steering coils must range from minus to plus  $B^*$ ,  $B^*$  being the field needed to completely remove the beam from the slits; for this reason the steering coils were biased. Double-wound coils were used; first winding gives a static field  $-B^*$ , while the second one gives a field varying from 0 to  $2B^*$ , so that the effective field covers the interval  $\pm B^*$ .

## 2. Microtron and beam characteristics

The microtron<sup>2)</sup> was working in the fundamental mode, at a cavity frequency of 2800 Mc/s and a magnetic field of 1 kG. The injection system is of the type suggested by Kapitza et al.<sup>3)</sup> The operating energy was

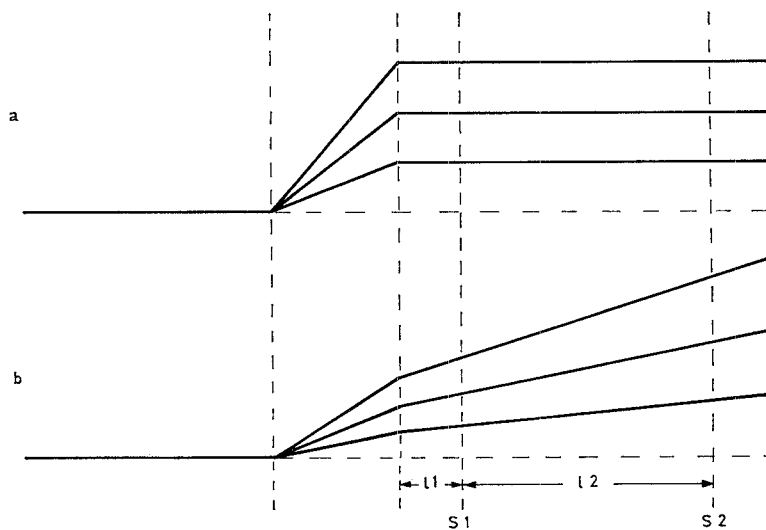


Fig. 4. Showing the method followed in the coils calibration.

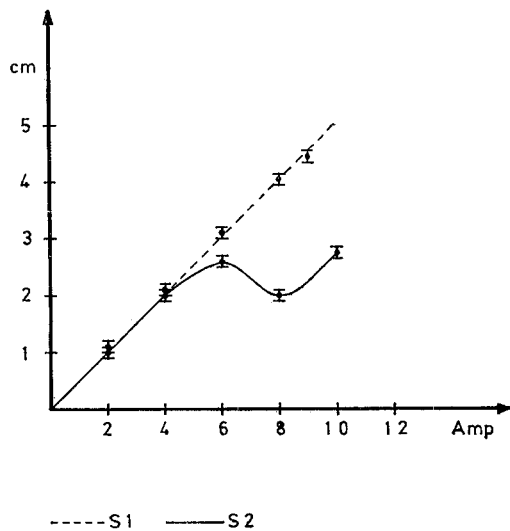


Fig. 5. Showing the principle of plane-parallel control.

10 MeV and the current on the last orbit was about 6 mA. The electron beam was extracted by means of an iron tube located to catch the beam tangentially to the last orbit. The perturbation caused by the tube was compensated by two parallel iron rods as suggested in<sup>4</sup>).

Special care has been taken to ensure stability of the microtron current: all measurements were taken after the system had been running for more than two hours, and the total current was checked at the start and at the end of each measurement.

### 3. Calibration of the system

The experimental apparatus was calibrated in several steps. First, the relationship between the current in the steering coils (4) and the deflection of the beam for a fixed energy was determined by measuring the displacement between the centers of the spots, obtained by taking a beam exposure for known values of the current in (4). The accuracy in the determination of such displacements is of the order of 0.5 mm, thus, with a distance of 170.5 cm between the centers of the coils (4) and the detection plane, the accuracy in the deflection angle is 0.3 mrad. The current in the coils was known to  $10^{-3}$  and stable to  $10^{-4}$ .

At the energy of 10 MeV the slope of the deflection characteristic was found to be:

$$\theta/I = (12.6 \pm 0.3) \text{ mrad/A.} \quad (1)$$

In a second step the coils (2) were series connected and a check was made on the mutual compensation, in order to have the beam displacement parallel to the incident direction.

The principle of the method is illustrated in fig. 4,

where (a) shows the case of complete compensation and (b) the case in which the second coil does not compensate the first one. The plots of the displacement of the spot centers in the section  $S_1$  and  $S_2$ , vs current, will have a linear behaviour with the same slope only in case (a).

We used this method to test the compensation of the steering coils. The position of the beam in sections  $S_1$  and  $S_2$  was recorded for several values of the current in the coils. The distance between the centers of the coils was 40.5 cm and the distances  $L_1$  and  $L_2$  were 30 cm and 230 cm respectively, so that the indeterminacy in the residual deflection was of the order of 0.5 mrad, the possible error in the location of the spot centers being 1 mm.

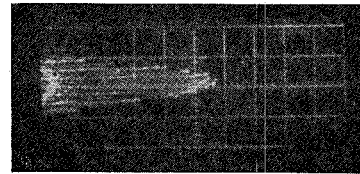


Fig. 6. Testing background effects.

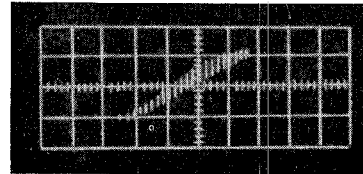
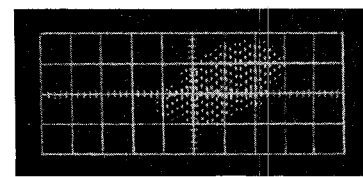
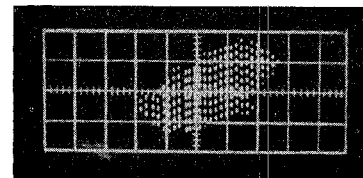


Fig. 7. Radial emittance (0.5 cm/cm; 12 mrad/cm).



Figs. 8 and 9. Vertical emittance (0.25 cm/cm; 2.4 mrad/cm).

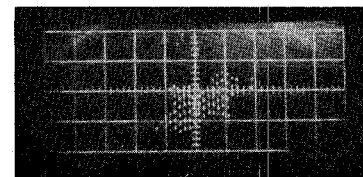


Fig. 10. As figs. 8 and 9, with 50% discriminator level.

The results shown in fig. 5 indicate that the compensation, in the range  $\pm 4$  A, corresponding to a displacement of the center of the beam of  $\pm 2$  cm, is good enough for our purposes. The relationship between the parallel displacement and the current in (4) is then:

$$\Delta Y/\Delta I = (5 \pm 1) \text{ mm/A.} \quad (2)$$

The effect of the background from the slits on the measurements has been evaluated in two ways. First, the beam was deflected through the steering coils (4) and a photo was taken of the pulse amplitude versus the steering current (fig. 6) for a fixed position of the beam on the slits (3). The photo shows the absence of a gaussian shape but rather a well defined interval of current beyond which the signal vanishes abruptly.

Second, two photos of beam emittance were taken changing the width of the slits from 0.5 to 2 mm in order to change the ratio width/thickness (which is responsible for background). In both cases the shape of the emittance is practically the same.

#### 4. Results

The experimental results are shown in figs. 7–10. Fig. 7 represents the distribution of the representative points in the radial phase plane: the resolution is 0.5 mm for the displacement and 0.3 mrad for the the angle. It is a picture of the emittance of the beam, for 95% of the total current that is 6 mA. Under these operation conditions the maximum values of position and angle are:

$$\begin{aligned} X_{\max} &= \pm 10 \text{ mm,} \\ X'_{\max} &= \pm 3.4 \text{ mrad.} \end{aligned} \quad (3)$$

Figs. 8 and 9 show the distribution in the vertical phase plane for 95% of the beam current, and refer to two different values of the rf tuning. In both cases the maximum values are

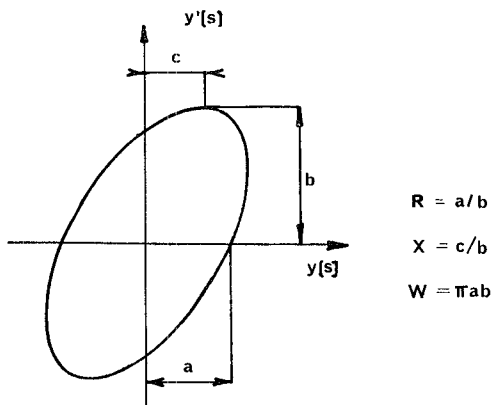


Fig. 11. Defining the ellipse parameters.

$$\begin{aligned} Z_{\max} &= \pm 5.3 \text{ mm,} \\ Z'_{\max} &= \pm 3.4 \text{ mrad.} \end{aligned} \quad (3a)$$

Finally, fig. 10 shows the situation in the vertical phase plane for 50% of the beam current ( $\approx 3$  mA).

The areas of the phase plane distributions shown in figs. 7 and 8, have been evaluated by direct integration from the enlarged photos (figs. 13 and 14), and were found to be

$$\begin{aligned} W_r &= 11 \text{ mrad} \cdot \text{cm} \quad (\text{radial plane}), \\ W_v &= 3.9 \text{ mrad} \cdot \text{cm} \quad (\text{vertical plane}). \end{aligned} \quad (4)$$

The photos show the emittance shapes in the plane defined by slit (2). In the assumption that the repre-

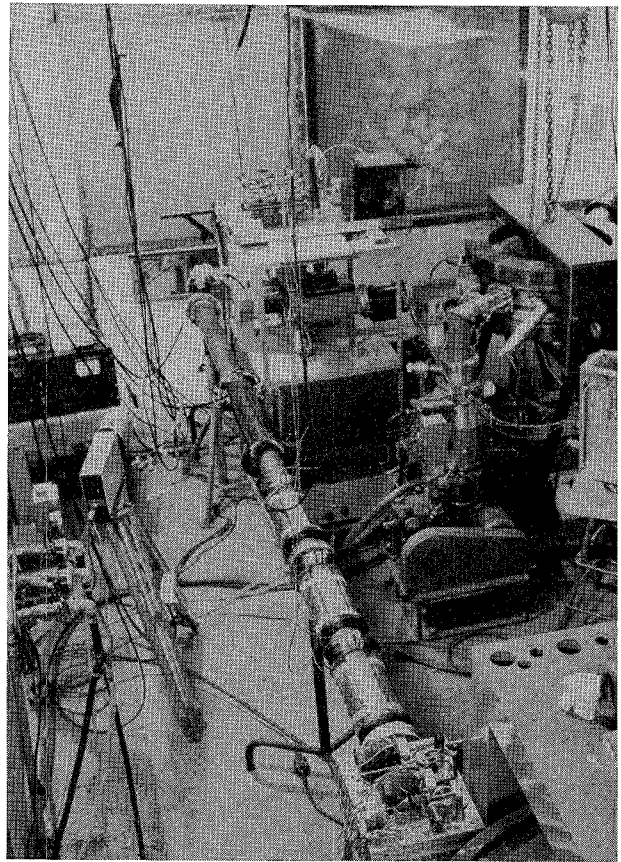


Fig. 12. General layout of the experiment.

sentative area can be limited by an elliptical closed curve and following the notations of Hereward<sup>5)</sup>, we determine the values of the three parameters  $R$ ,  $X$  and  $W$ , which completely define the ellipses (fig. 11) at the output plane of the machine. Applying the transformation rules<sup>6)</sup> for  $R$  and  $X$  from the plane of measurement back to the machine (drift space length = 0.80 m) we obtain at the output plane of the machine:

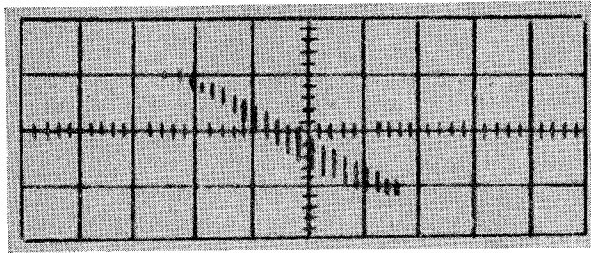


Fig. 13. Photo of fig. 7 magnified.

Radial plane	Vertical plane
$R = 0.154,$	$R = 0.95,$
$X = -0.10 \text{ m},$	$X = -0.10 \text{ m},$
$W = 11 \text{ mrad} \cdot \text{cm},$	$W = 3.9 \text{ mrad} \cdot \text{cm}.$

The starting values  $R$  and  $X$  used in the transformation were determined from the experimental distributions (figs. 13 and 14) fitted with ellipses of area equal to the measured values of eq. (4). The beam current associated to the ellipse defined in this way is of the order of 95% of the current of the initial distribution ( $\approx 5.0 \text{ mA}$ ). Fig. 12 gives an overall view of the experiment.

After having sent this article, it came to our knowledge that an analogous system had been proposed by

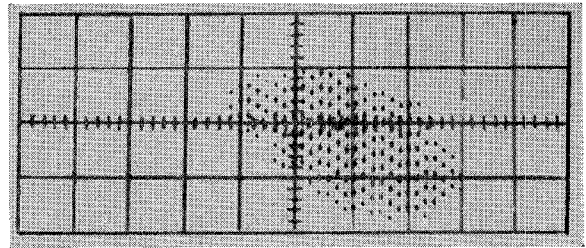


Fig. 14. Photo of fig. 8 magnified.

Vosicki (Proc. 1966 Linear Accelerator Conference, Los Alamos).

It is a pleasure to thank Prof. U. Bizzarri for continuous help and criticism, and Dr. A. Vignati for his assistance in microtron operation.

#### References

- 1) A. van Steenbergen, 5<sup>th</sup> Intern. Conf. *High-energy accelerators*, Frascati (1965) p. 311.
- 2) U. Bizzarri and A. Vignati, Laboratori Nazionali di Frascati, Report LNF-67/46 (1967).
- 3) S. P. Kapitza et al., *Sovj. Phys. JETP* **12** (1961) 693.
- 4) H. Reich and K. Lons, *Nucl. Instr. and Meth.* **31** (1964) 221.
- 5) H. G. Hereward, CERN Report PS/Int. TH 59-5 (1959).
- 6) M. Bassetti, R. M. Buonanni and M. Placidi, *Nucl. Instr. and Meth.* **45** (1966) 93.